Development/Plasticity/Repair

Effects of Neurotoxic and Neuroprotective Agents on Peripheral Nerve Regeneration Assayed by Time-Lapse Imaging *In Vivo*

Y. Albert Pan, Thomas Misgeld, Jeff W. Lichtman, and Joshua R. Sanes
Department of Anatomy and Neurobiology, Washington University Medical School, St. Louis, Missouri 63110

A direct histological assay of axonal regeneration would have many advantages over currently available behavioral, electrophysiological, and radiometric assays. We show that peripheral sensory axons marked with the yellow fluorescent protein in transgenic mice can be viewed transcutaneously in superficial nerves. Degenerating and regenerating axons can be followed in live animals with a dissecting microscope and then, after fixation, studied at high resolution by confocal microscopy. Using this approach, we document differences in regenerative ability after nerve transection, crush injury, and crush injury after a previous "conditioning" lesion. We also show that the chemotherapeutic drug vincristine rapidly but transiently blocks regeneration and that the immunosuppressive drug FK506 modestly enhances regeneration. Moreover, FK506 nearly restores normal regenerative ability in animals treated with submaximal doses of vincristine. Because neuropathy is the major dose-limiting side effect of vincristine, we propose that its efficacy could be enhanced by coadministration of FK506 analogs that are neuroactive but not immunosuppressive.

Key words: **regeneration; conditioning lesion; FK506; transgenic mice; vincristine; Wallerian degeneration**

Introduction

After transection of a mammalian peripheral axon, the distal segment, separated from its soma, degenerates in a series of steps called Wallerian degeneration. After a "waiting period," the axon then extends from the proximal cut end; in favorable cases, it reaches and reinnervates its original target, leading to nearly perfect restoration of function. These processes of degeneration and regeneration have been studied in detail because they provide an accessible model of axonal growth and guidance, because peripheral nerve injuries and neuropathy are prevalent in clinical practice, and because understanding why regeneration is so successful in the peripheral nervous system may shed light on why it is so poor in the CNS (for review, see Ramon y Cajal, 1928; Young 1942; Guth, 1956; Fawcett and Keynes, 1990; Griffin and Hoffman, 1993; Sanes and Jessell, 2000).

Despite intensive study, however, many questions remain, not only about the molecular control of degeneration and regeneration but even about the sequence and pace of the cellular events that underlie loss and return of function. Moreover, although many molecules and interventions have been shown to speed or slow recovery after nerve injury (Boyd and Gordon, 2003; Cui et al., 2003; Kim et al., 2003; McMurray et al., 2003; Meiners and Mercado, 2003; Murakami et al., 2003; Van der Zee et al., 2003), it is unclear in most cases whether these agents affect the waiting period before regeneration begins, the speed of axonal regeneration, the number of axons that regenerate, or some other variable. Results of such studies are therefore less than optimally useful either for analyzing regenerative mechanisms or for designing therapies. To a large extent, these difficulties reflect a methodological problem: currently available methods for monitoring the degeneration and regeneration of injured peripheral nerves are cumbersome or indirect (for review, see Frykman et al., 1988). For example, the speed of regeneration can be determined by counting axons at multiple distances from a site of injury, but it is difficult to process the large numbers of sections required. Alternatively, recovery of sensory or motor function can be assayed behaviorally (commonly by sensitivity to tactile stimuli or by extent of toe spreading) or physiologically (for example, by return of muscle action potentials), but regeneration rate is only one of a host of factors that influence the return of function. Yet another method measures the distance that radioactively labeled proteins are transported, but size and number of regenerated axons indistinguishably influence these measurements.

More useful assays would allow visualization of degenerating and regenerating axons in whole nerves. In the first part of this paper, we report the development of such assays based on use of transgenic mice that express spectral variants of the green fluorescent protein (GFP) (together called XFPs) in their peripheral axons (Feng et al., 2000). We then go on to use these assays to address some outstanding questions about a protocol known to speed regeneration (the conditioning lesion) (McQuarrie et al., 1977; Forman et al., 1980; Sjoberg and Kanje, 1990; Lankford et al., 1998; Neumann and Woolf, 1999; Qiu et al., 2002) and two drugs that have clear effects on functional recovery after nerve

Received Aug. 26, 2003; revised Oct. 19, 2003; accepted Oct. 22, 2003.

This work was supported by grants from the National Institutes of Health (NIH) to J.W.L and J.R.S, by a fellowship from the Deutsche Forschungsgemeinschaft to T.M., and by an institutional National Research Service Award training grant from NIH to Y.A.P. We thank Dr. Susan Mackinnon for advice.

Correspondence should be addressed to Joshua R. Sanes, Department of Anatomy and Neurobiology, Washington University Medical School, St. Louis, MO 63110. E-mail: sanesj@pcg.wustl.edu.

 0270-6474/03/2311479-10$15.00/0

injury but for which effects on axonal behavior remain unclear: vincristine (Bradley et al., 1970; Shiraishi et al., 1985; Tanner et al., 1998; Nakamura et al., 2001) and FK506 (Lyons et al., 1994; Gold et al., 1995; Lee et al., 2000; Gold and Villafranca, 2003).

Materials and Methods

Mice. We used XFP transgenic mice in which GFP or one of its spectral variants is expressed in some or all sensory and motor axons under the control of regulatory elements from the mouse *thy-1* gene (Feng et al., 2000). In most of the experiments described here, we used adult yellow fluorescent protein (YFP)-H mice weighing 20–30 gm. The YFP-H line is available to academic researchers from the Induced Mutant Resource at The Jackson Laboratory (Bar Harbor, ME).

Surgical procedures. Mice were anesthetized by subcutaneous injection of ketamine and xylazine. The hindlegs or back were depilated by shaving and applying Nair lotion (Carter Products, New York, NY). The saphenous nerve was viewed transcutaneously under an SZX12 fluorescence dissecting microscope (Olympus Optical, Tokyo, Japan), and a cut (~1 mm) was made in the skin to expose the nerve. We then cut the exposed nerve with scissors or crushed it with fine forceps. This incision was so small that it did not need to be closed with sutures. Dorsal cutaneous nerves were reached through a larger incision in the skin along the dorsal midline, which was closed with 6-0 sterile sutures. At the terminal experiment, mice were killed with an injection of sodium pentobarbital.

Drug administration. Vincristine sulfate (Sigma, St. Louis, MO) was diluted to 75 μg/ml in 0.9% NaCl and injected intraperitoneally. FK506 (provided by Fujisawa, Deerfield, IL) was diluted to 600 μg/ml and injected subcutaneously at doses indicated in the figures.

Measuring the rate of regeneration. For *in vivo* transcutaneous imaging of the saphenous nerve, we crushed the saphenous nerve near the groin and crushed again at the same place 3 d afterward. The tips of forceps were dipped in 1 μm orange FluoSpheres (Molecular Probes, Eugene, OR) to mark the crush site. For imaging in live animals, animals were anesthetized and placed directly under the fluorescence dissecting microscope. Images were captured with a cooled CCD camera. For high-resolution imaging, nerves were fixed in 4% paraformaldehyde for 60 min, rinsed, mounted in Vectashield (Vector Laboratories, Burlingame, CA), and viewed with a Bio-Rad MRC-1024 confocal microscope (Bio-Rad, Hercules, CA).

Results

Imaging peripheral axons in live mice

We previously characterized transgenic mice in which GFP or one of its spectral variants is strongly expressed in projection neurons (Feng et al., 2000; Keller-Peck et al., 2001; Nguyen et al., 2002). We began the present study by asking whether labeling was sufficiently intense that peripheral axons could be viewed transcutaneously in adult mice using a dissecting microscope equipped for fluorescence. Indeed, once the hair was removed, superficial nerves were visible in live animals. Figure 1*a* shows the depilated leg of an anesthetized adult mouse of line YFP-H viewed under fluorescence optics. The saphenous, a sensory nerve, was visible through the skin from the groin to the ankle. Smaller branches that left the main trunk to terminate in the skin were also visible. After this image was captured, the mouse was killed, the skin was removed, and the same area was reimaged (Fig. 1*b*). The similarity of the two images indicates that the skin obscures few details of nerve structure. Similar results were obtained with three other transgenic lines [YFP-16, RFP-8 (red fluorescent protein-8), and GFP-I] (Feng et al., 2000), but labeling was most intense with YFP-H, so this line was used in subsequent studies.

In YFP-H mice, a subset of sensory neurons expresses YFP at high levels, and most of the others are completely YFP negative (Feng et al., 2000). This pattern allowed us to resolve small groups

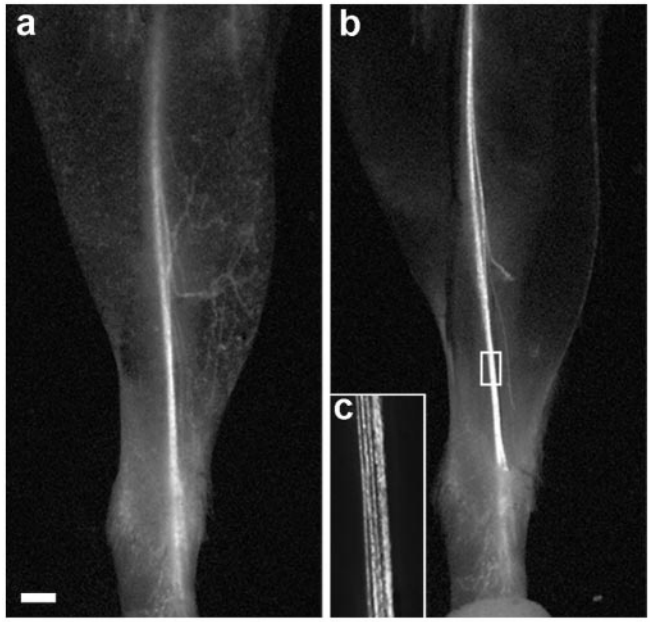

Figure 1. Transcutaneous imaging of the saphenous nerve. *a*, The leg of a YFP-H transgenic mouse imaged with a fluorescence dissecting microscope after depilation. The saphenous nerve and some of its cutaneous branches are visible. *b*, After the image in *a* was captured, the mouse was killed, the skin was removed, and the leg was imaged again. The boxed area in *b* is shown at higher magnification in *c*. Scale bar, 1 mm.

of labeled sensory axons in the saphenous (Fig. 1*c*), suggesting that it might be possible to visualize individual YFP-positive axons in favorable preparations. Studies of two other peripheral nerves confirmed that this was the case. First, labeling was clearly visible transcutaneously in the pinna of the ear, in which fine nerve branches containing only a few axons run directly beneath a thin epidermal layer (Fig. 2*a*). Combined fluorescence and bright-field imaging shows that many but not all nerve branches are associated with blood vessels (Fig. 2*b*), suggesting that this preparation may be useful for investigating the mechanism of this association (Mukouyama et al., 2002). Reexamination by confocal microscopy, after the animal was killed and the skin removed, showed that many of the branches contained only a single labeled axon (Fig. 2*c*). Second, YFP-positive axons could be followed over distances of >1.5 cm in the dorsal cutaneous nerves that arise from the thoracic and lumbar segments of the spinal cord and deliver sensory axons to the skin of the back (Fig. 2*d*). These nerves are small, and there were generally fewer than 10 labeled axons per nerve in YFP-H mice. Therefore, we were able to identify individual axons within the nerves (Fig. 2*e*). To confirm that the YFP-positive structures were indeed individual axons, we sectioned an adjacent segment of the nerve shown in Figure 2*e* and stained the section with anti-laminin to mark the endoneurial tubes that ensheath individual axons (Fig. 2*f*). Examination of the sections by confocal microscopy showed that each YFP-positive structure occupied a single endoneurial tube and was therefore a single axon (Fig. 2*g*). These nerves are not visible transcutaneously, but they have the advantage for regeneration studies that they are numerous. Therefore, we were able to exclude nerves with too many labeled axons to distinguish clearly and still obtain data from approximately eight nerves per animal.

Degeneration and regeneration of YFP-labeled axons

To assay peripheral regeneration, we cut or crushed the saphenous or dorsal cutaneous nerves, waited varying intervals, and

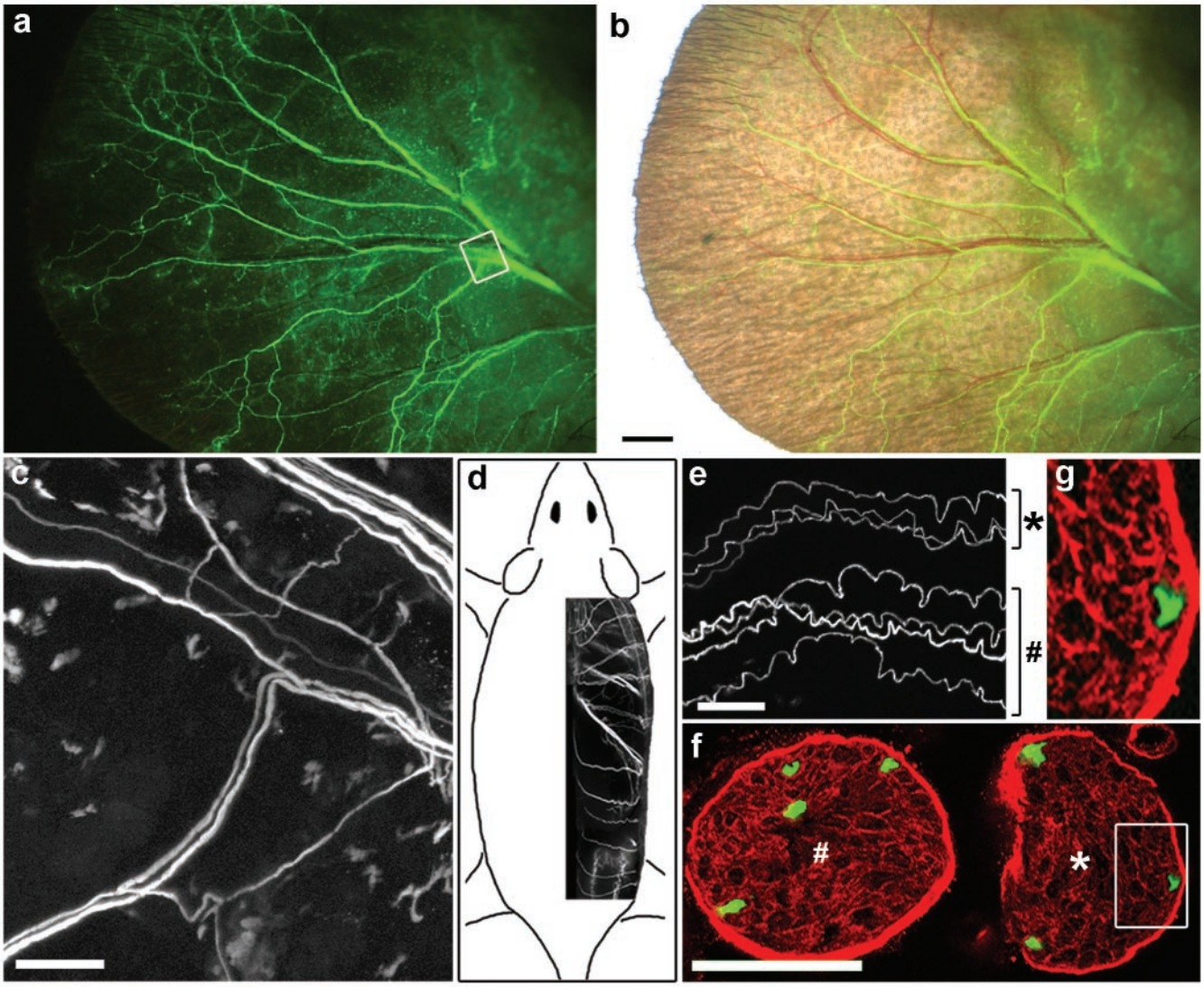

Figure 2. Imaging individual axons in the ear (*a–c*) and dorsal cutaneous nerves (*d–g*) of YFP-H mice. *a*, The pinna of the ear of a live mouse. Small bundles of YFP-positive axons are clearly visible. *b*, Fluorescence image overlaid on a bright-field view. Some but not all axon bundles are apposed to blood vessels. *c*, After the images in *a* and *b* were captured, the animal was killed, the skin was peeled off, and the area boxed in *a* was imaged again on the confocal microscope to show that individual axons had been visible in the live animal. *d*, Dorsal cutaneous nerves inserted in a sketch to show their position. *e*, Confocal image of individual axons in a fixed dorsal cutaneous nerve. *f*, A region adjacent to that in *e* was frozen, sectioned, and stained with anti-laminin. The seven axons visible in the whole mount are all seen in the section. Symbols (* and #) mark corresponding nerves in *e* and *f*. *g*, The area boxed in *f* is shown at higher magnification to demonstrate that the YFP-positive structure occupies a single laminin-rich endoneurial tube and is therefore a single axon. Scale bars: *b*, 1 mm; *c*, *e*, 100 μm; (in *f*) *f*, 50 μm, *g*, 23 μm.

then killed the mice, fixed the nerves *in situ*, dissected them free, mounted them on slides, and obtained confocal images. After complete transection of either nerve ("nerve cut"), YFP-positive axons in the distal stump retained a fluorescent core and thus appeared intact for ~1 d (Fig. 3*a*). During the subsequent day, however, they began to fragment (Fig. 3*b*). The YFP-rich remnants resembled the "ovoids" described in previous studies of Wallerian degeneration (Ramon y Cajal, 1928; Gutmann and Holubar, 1950; Lubinska, 1977; Stoll et al., 1989). These YFP-rich deposits became smaller and fewer in number over the next several days (Fig. 3*c*,*d*), but a few persisted for >1 week.

Regeneration after nerve cut was limited. During the first 4 d after injury, axons formed thick, club-shaped endings just proximal to the site of injury, but only a few grew beyond this site (Fig. 3*e*, top nerve). Additional outgrowth occurred over the next few days (Fig. 3*f*), but even 2 weeks after transection, only a minority of the cut axons had regenerated a significant distance, and many of these escaped into neighboring connective tissue (Fig. 3*g*,*h*). Therefore, regeneration after nerve transection was inefficient, poorly oriented, and variable from animal to animal. In contrast, regeneration after crush injury was efficient, well oriented, and reproducible from animal to animal. These differences are consistent with both clinical and experimental studies in which recovery is more complete after a crush than after complete transection (Young 1942; Dagum et al., 1998; Nguyen et al., 2002). The contrast is apparent in Figure 3*e*, which shows two branches of the saphenous nerve 4 d after injury. One branch had been crushed (bottom) and the other had been cut (top). After nerve crush, many axons began growing past the site of injury within 1–2 d, and most of the damaged axons extended past the site of injury within the next few days (Fig. 3*e*). Imaging of dorsal cutaneous nerves after crush injury confirmed that nearly all labeled axons grew into the distal stump (Fig. 3*i*,*j*).

For multiple time point analysis of nerve regeneration, we used the saphenous nerve because it can be imaged transcutaneously. The nerve was viewed under the fluorescence dissecting

microscope, a small incision was made in the skin, and the nerve was crushed with fine forceps. Because the nerve was visible before the skin was incised, it was possible to limit the incision to ~1 mm so that bleeding was inconsequential and no sutures were required. To mark the site of injury accurately, we dipped the forceps in a slurry of ~1 μm fluorescent beads, which adhered to epineurial connective tissue and could be seen transcutaneously for >1 week. At daily intervals after axotomy, the mouse was lightly anesthetized and viewed under the fluorescence dissecting microscope. We expected that the distance from the beads to the distal-most front of YFP would correspond to the extent of regeneration; however, no clear distal boundary of fluorescence was visible (Fig. 4*a*). The explanation was that regeneration into the distal stump occurred before YFP-positive debris from damaged axons had been cleared (Figs. 3*a–e*, 4*b*); although degenerating and regenerating axons can be distinguished readily at high magnification (Fig. 4*c*), they cannot be distinguished transcutaneously. As a means of delaying regeneration until most axonal remnants in the distal stump had been removed, we crushed the nerve a second time, 3 d after the first injury. Using this protocol, we were able to identify regenerating axons transcutaneously and follow the progress of regeneration noninvasively (Fig. 4*d*). Reviewing after removal of the skin confirmed that the front of fluorescence viewed transcutaneously corresponded to the distal-most extent of regeneration (Fig. 4*e–g*).

In summary, the YFP mice provide a suite of assays for analyzing peripheral nerves. Two preparations can be used for multiple time point noninvasive imaging: the pinna of the ear to monitor stability of axons and the saphenous after two successive crushes to monitor regeneration. In both cases, specimens can be fixed after imaging and reexamined at high magnification by confocal microscopy. Two other assays are not suited for time-lapse imaging but provide valuable data on axonal degeneration and regeneration: the dorsal cutaneous to monitor individual axons and the singly crushed saphenous to monitor many axons at once. In the sections that follow, we report use of these assays to test effects of treatments that have been reported to affect functional recovery after nerve injury.

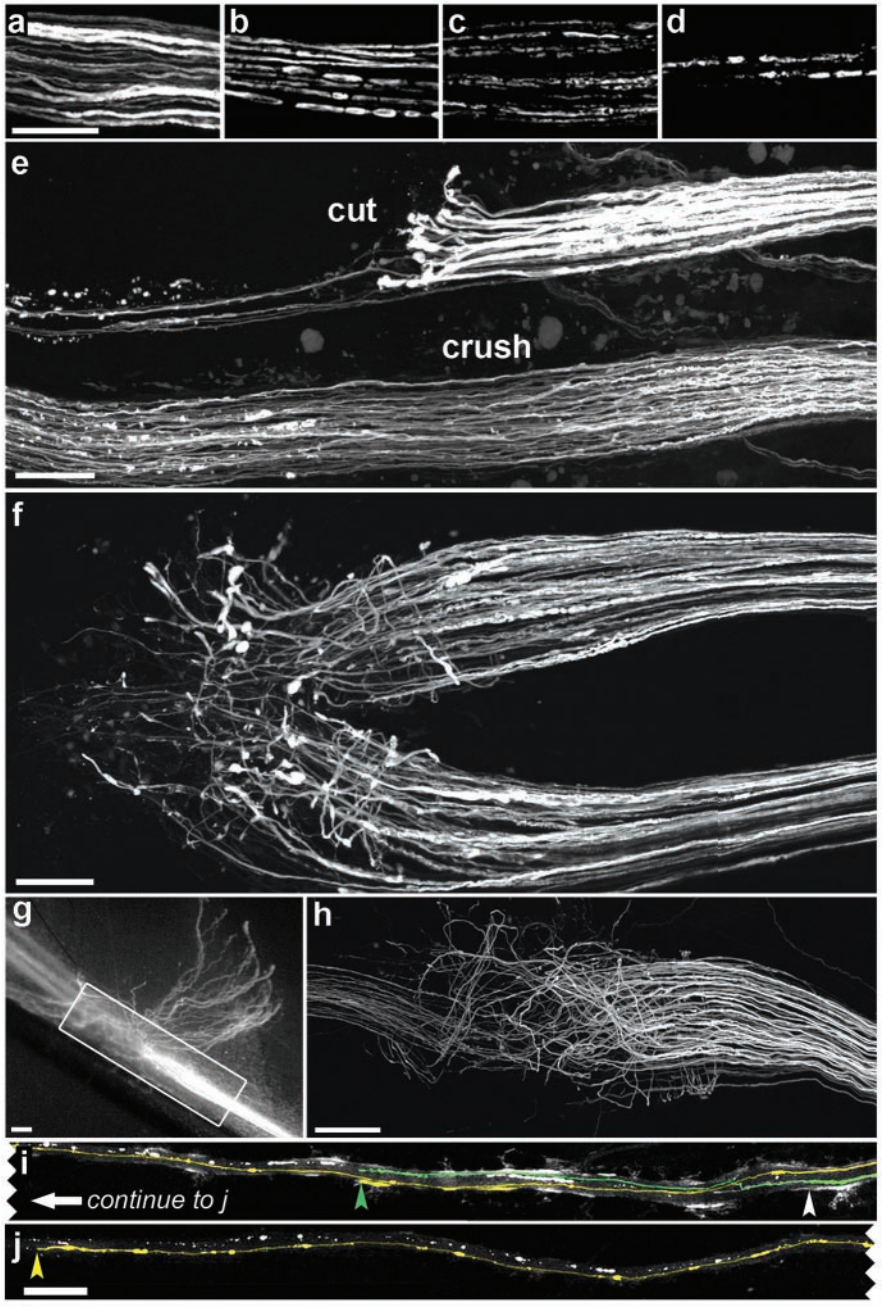

Figure 3. Degeneration and regeneration of YFP-positive axons in the saphenous (*e–h*) and dorsal cutaneous (*a–d, i, j*) nerves. All panels show confocal images except *g*, which is from a dissecting microscope. Proximal is to the right in all parts. *a–d*, Distal stumps 1 d (*a*), 2 d (*b*), 3 d (*c*), or 5 d (*d*) after transection. YFP-positive axons fragment into ovoids in ~2 d, some of which persist for >5 d. *e*, Two branches of the saphenous, 4 d after the top branch had been cut and the bottom had been crushed. Axons thickened after nerve cut and formed club-shaped endings; only a few regenerated into the distal stump (to the left). In contrast, axonal regeneration is advanced after crush injury. *f*, Six days after the cut, numerous sprouts extend past the site of damage, but they are disordered. *g*, *h*, Two weeks after the cut, numerous axons have regenerated, but many of these grow blindly into connective tissue (*g*), and only a subset grows in the distal stump. *i*, *j*, Adjacent portions of the same dorsal cutaneous nerve were imaged 5 d after it was crushed (white arrowhead). There were only two labeled axons in this dorsal cutaneous nerve, both of which have regenerated. The axons are pseudocolored and end at the arrowhead of the corresponding color. White slashes are debris from degenerating YFP-positive axons. Scale bars: *a–h*, 100 μm; *j*, 250 μm.

Effects of a conditioning lesion

Nerve regeneration after axotomy is speeded if the nerve has suffered a previous injury (McQuarrie et al., 1977; Forman et al., 1980; Sjoberg and Kanje, 1990). The stimulatory effect of the first or conditioning lesion is well described, but its cellular basis is not clear. The protocols described above, in which the saphenous nerve was crushed either once or twice, provided a way to assess the effects of conditioning lesion.

After a single crush, the speed of axonal regeneration in the saphenous nerve increased progressively over a period of 3–4 d.

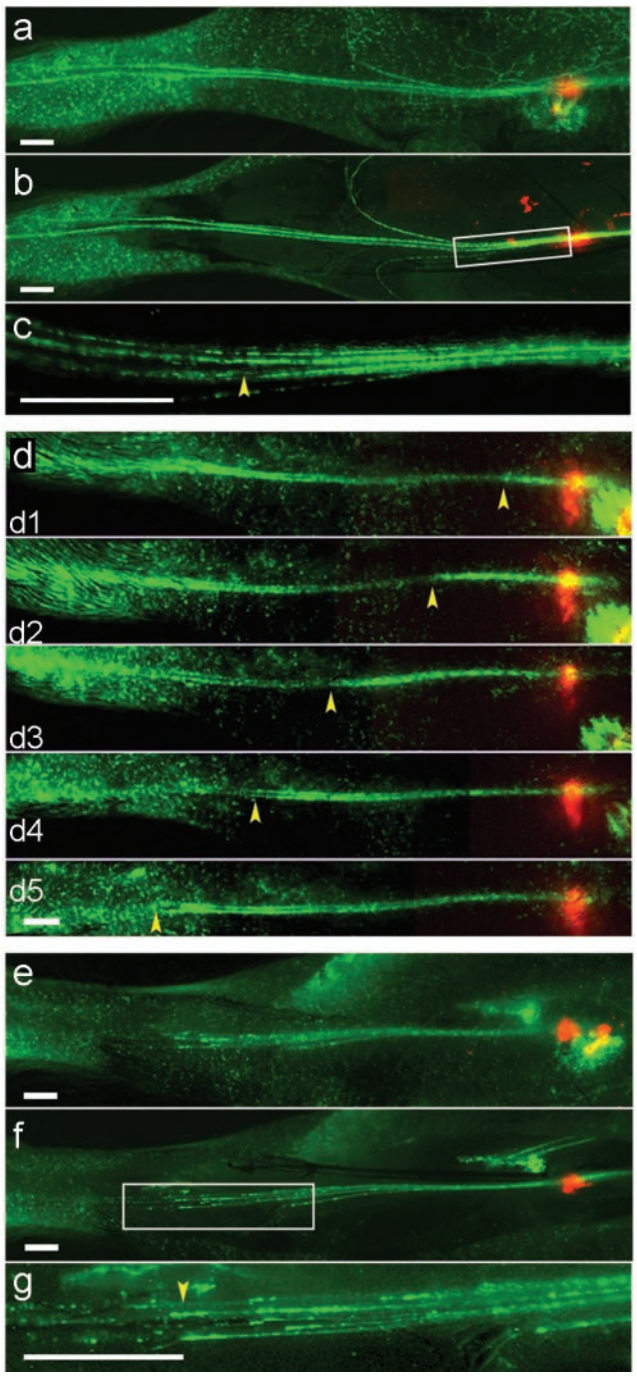

Figure 4. Imaging regeneration in live mice after crush injury to the saphenous nerve. Crush sites are indicated by deposits of orange microspheres, and proximal is to the right. Images were captured from a dissecting microscope transcutaneously (*a, d, e*) or after killing the mice and removing the skin (*b, c, f, g*). *a–c*, Three days after a single crush, regeneration is difficult to assess transcutaneously (*a*). Imaging after removal of skin shows that this is because regenerating axons are intermingled with fluorescent remains of degenerating axons (*b, c*). The region boxed in *b* is shown at higher power in *c*. *d*, When regeneration is delayed by a double-crush protocol, debris has been cleared by the time regeneration occurs, so the front of regeneration (yellow arrowheads) is easily discerned. *d1–d5*, 1–5 d after second crush. *e–g*, The front of fluorescence was viewed transcutaneously in another mouse 5 d after the second of two nerve crushes (*e*), and then the mouse was killed, the skin was removed, and the same area was imaged again (*f*). The region boxed in *f* is shown at higher power in *g*. The extent of regeneration measured live accurately reflects tips of fastest-regenerating axons (arrowhead). Scale bars, 1 mm.

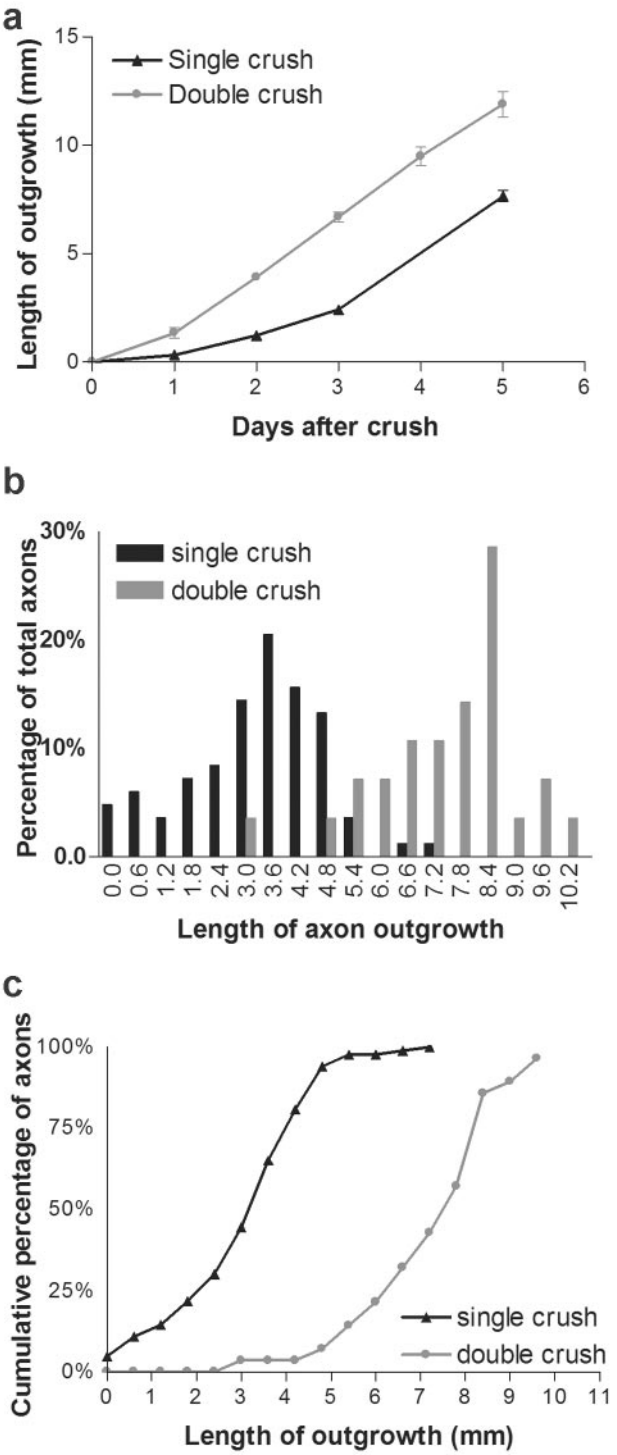

Figure 5. Effect of a conditioning lesion on regeneration after nerve crush. *a*, Extent of regeneration in the saphenous nerve after a single nerve crush or the second of two crushes. Measurements were made as shown in Figure 4*d–g*. Points and bars show mean ± SEM ($n = 4–8$). *b*, Regeneration of single axons in dorsal cutaneous nerves 5 d after a single nerve crush or the second of two crushes. Measurements were made as shown in Figure 3, *i* and *j* ($n = 83$ axons for single crush and 28 for double crush). *c*, Cumulative frequency plot of data from *b*. The difference between curves is significant at $p < 0.01$ by Kolmogorov–Smirnov test.

The average rate was 0.3, 1.2, and 2.4 mm/d on the first, second, and third days, respectively, after injury and reached 2.7 mm/d between days 3 and 5 (Fig. 5*a*). The lag period and final rate are similar to those reported previously (Gutman et al., 1942;

McQuarrie et al., 1977; Danielsen et al., 1986). In contrast, axons regenerated 1.3 mm/d during the first day after the second of two injuries, the rate increased to 2.6 mm/d on the second day, and the rate remained 2.4–2.8 mm/d over the next 3 d. Thus, a main difference between the responses to a single injury and to the second of two injuries is that regeneration reaches its maximum rate sooner in the latter case; however, the maximum rate does not differ significantly between the two protocols.

The front of fluorescence in the regenerating saphenous primarily reflects the position of the fastest-growing axons, so our measurements may not be representative of most axons in the nerve. To obtain information about variation among axons, we measured the length of single regenerating axons in the dorsal cutaneous nerves after either a single or double crush (Fig. 5*b*). Because these nerves could not be imaged repeatedly, we limited our observations to a single time point, 5 d after the final injury. Three main results emerged from analyzing the dorsal cutaneous nerves and from comparing them to the saphenous. (1) Rates of regeneration varied greatly among axons. Five days after a single crush, some axons had regenerated 7 mm, whereas others had not extended past the crush site; the SD was nearly half the mean (3.2 ± 1.5 mm; mean ± SD; n = 83 axons). The range (3.2–10.3 mm) and the variation around the mean (7.2 ± 1.6; n = 28) were similarly high after double crush. (2) As expected, rates of regeneration measured in the saphenous nerve were similar to those of the fastest-growing axons in the dorsal cutaneous. Five days after a single crush, the extension measured in the saphenous was 7.7 mm, which was similar to the longest-regenerated axon in the dorsal cutaneous (7 mm). Corresponding lengths 5 d after the second of two crushes were 11.9 mm for the saphenous and 10.3 mm for the dorsal cutaneous. (3) The extent of regeneration was increased for the entire population of doubly crushed axons, not just those that extended farthest. The generality of the effect is seen most clearly by plotting the cumulative frequency of axons that had regenerated less than a given distance after a single or double crush: the two curves are nearly parallel, with the latter shifted to the right (Fig. 5*c*).

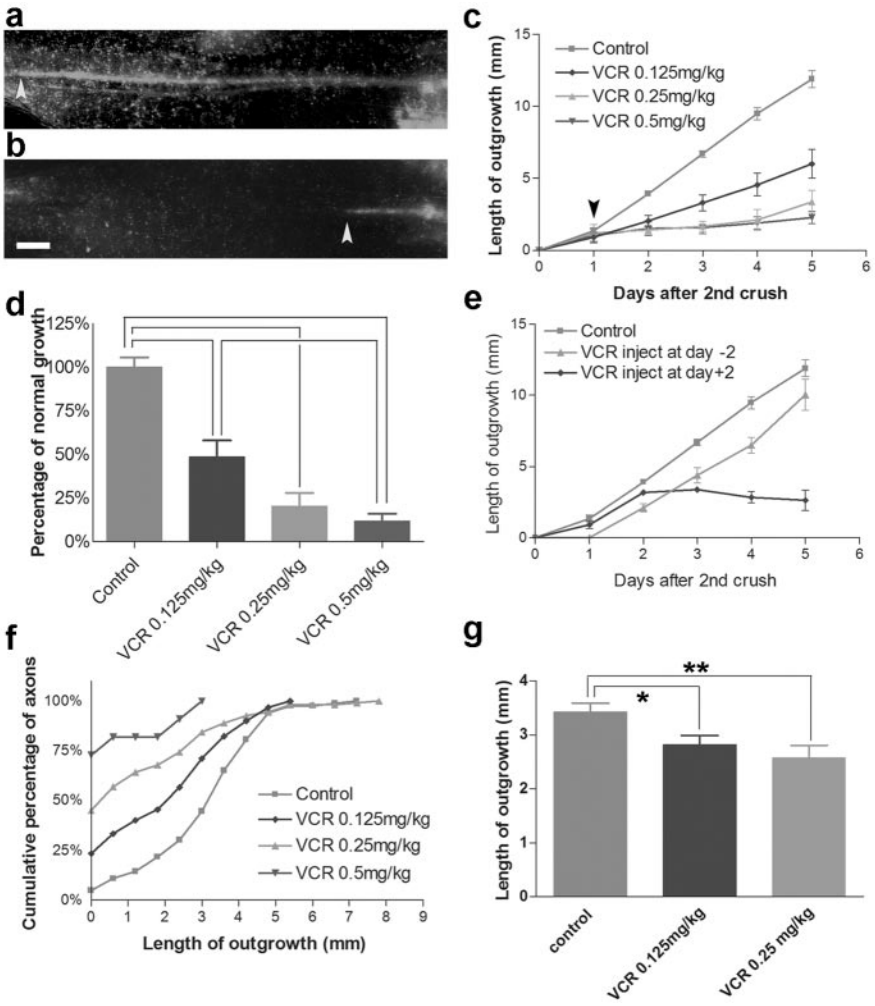

Figure 6. Inhibition of regeneration by vincristine. *a*, *b*, Regeneration in the saphenous 5 d after the second of two nerve crushes in an untreated mouse (*a*) or a mouse that had received a single injection of 0.5 mg/kg vincristine 4 d previously (*b*). Arrowheads mark the extent of regeneration. Scale bar, 1 mm. *c*, *d*, Dose-dependent inhibition of regeneration by vincristine, measured as in *a*, *b*. The arrow in *c* indicates the time of vincristine injection. Points and bars show mean ± SEM (n = 6–12). Values in *d* are calculated from the data in *c*, on the basis of the extension during the 4 d after administration of vincristine. Differences between pairs of bars connected by brackets are significant at $p < 0.01$ by t test. *e*, Inhibition of regeneration by vincristine is rapid but transient. Experiments were as in *a*–*c*, but the time of vincristine administration (0.25 mg/kg) was either 2 d before (day −2) or 2 d after (day +2) the second crush. *f*, *g*, Effects of vincristine on regeneration of single axons in the dorsal cutaneous nerve. The cumulative frequency plot in *f* shows a dose-dependent increase in the number of axons that fail to regenerate. Lengths of those axons that did regenerate (*g*) are also decreased by vincristine. The difference between curves in *f* is significant at $p < 0.05$ by Kolmogorov–Smirnov test. In *g*, *$p = 0.01$; **$p = 0.002$.

Effects of vincristine

Vincristine, an inhibitor of microtubule formation, inhibits functional recovery after peripheral nerve injury (Shiraishi et al., 1985; Ruigt and den Brok, 1995; Nakamura et al., 2001; Paydarfar and Paniello, 2001), but its effects on axonal regeneration per se are unclear. To address this issue, we first assessed the effects of vincristine on regeneration of the saphenous nerve using the conditioning lesion protocol described above. The doses that we used (0.125–1.25 mg/kg) corresponded to the range used in the studies cited above. As shown in Figure 6*a*–*c*, a single dose of vincristine administered intraperitoneally 1 d after the second nerve crush promptly decreased the rate of regeneration. The effect of vincristine was dose dependent, with an ~50% decrease at the lowest dose tested and nearly complete inhibition at the highest (Fig. 6*d*).

Regeneration was slightly faster on the fourth day after treatment (that is, the fifth day after injury) with a submaximal dose of vincristine (0.25 mg/kg) than on the first 3 d (Fig. 6*c*), suggesting that axons might begin recovering from vincristine treatment after several days. To test whether regeneration rate increased at a set time after vincristine treatment, we administered vincristine (0.25 mg/kg) 2 d before the second crush. This was 2 d after the first crush; thus, as in the experiment described above, the drug was administered after axotomy. In this series, regeneration was delayed by 1 d but then resumed at a speed similar to that in

untreated nerves (Fig. 6*e*). Thus, effects of vincristine are of limited duration. We also asked whether the rapidity with which vincristine affects regeneration depends on its being administered soon after damage; however, even when vincristine was administered after regeneration was well under way, it promptly blocked additional outgrowth (Fig. 6*e*).

To assess the effect of vincristine on individual axons, we used the dorsal cutaneous nerves. In this series, vincristine was administered once, 1 d after a single nerve crush. Analysis of the dorsal cutaneous nerves (Fig. 6*f*,*g*) confirmed the dose-dependent inhibition documented in the saphenous and also provided two novel results: (1) vincristine inhibits regeneration to a similar extent after a single nerve crush (dorsal cutaneous) or repeated injury (saphenous), and (2) in addition to decreasing the rate of regeneration, vincristine decreases the fraction of axons that regenerate at all. In untreated animals, only 5% of labeled, crushed axons in the dorsal cutaneous nerves failed to regenerate >300 μm beyond the site of injury over a period of 5 d; this percentage increased to 23, 45, and 75% after administration of 0.125, 0.25, and 0.5 mg/kg vincristine, respectively. Together, results from the saphenous and dorsal cutaneous nerves show that vincristine has two separate effects on regenerating axons, preventing outgrowth of some and slowing others.

Because repeated application of vincristine leads to neuropathy in rodents (Aley et al., 1996; Tanner et al., 1998), we asked whether the single dose used in our studies led to loss of axons, which would complicate interpretation of results on regeneration. Transcutaneous imaging of the saphenous showed that the proximal stump persisted after nerve damage, and the short segment that regenerated before vincristine administration persisted after administration (Fig. 6*a*,*b*). We also examined the pinna of the ear because it allowed repeated imaging of individual axons. In fact, no loss, rerouting, or sprouting of axons was observed during the 3 d after administration of vincristine (Fig. 7*a–d*). Therefore, consistent with the result that inhibition of regeneration by vincristine is transient, the lack of regeneration after its administration is not secondary to loss of axons. On the other hand, when intact YFP-positive dorsal cutaneous axons were viewed at high power in the confocal microscope, vacuolation and ruffling were apparent in vincristine-treated mice but not in controls (Fig. 7*e*,*f*). Similar but more pronounced defects were apparent in the proximal segments of axon that had been crushed (Fig. 7*g*,*h*). These abnormalities, which are consistent with ultrastructural defects reported after multiple doses of vincristine (Tanner et al., 1998), suggest that vincristine acts to disrupt axonal integrity in a way that blocks regeneration after a single dose and may eventually lead to axonal loss after repeated administration.

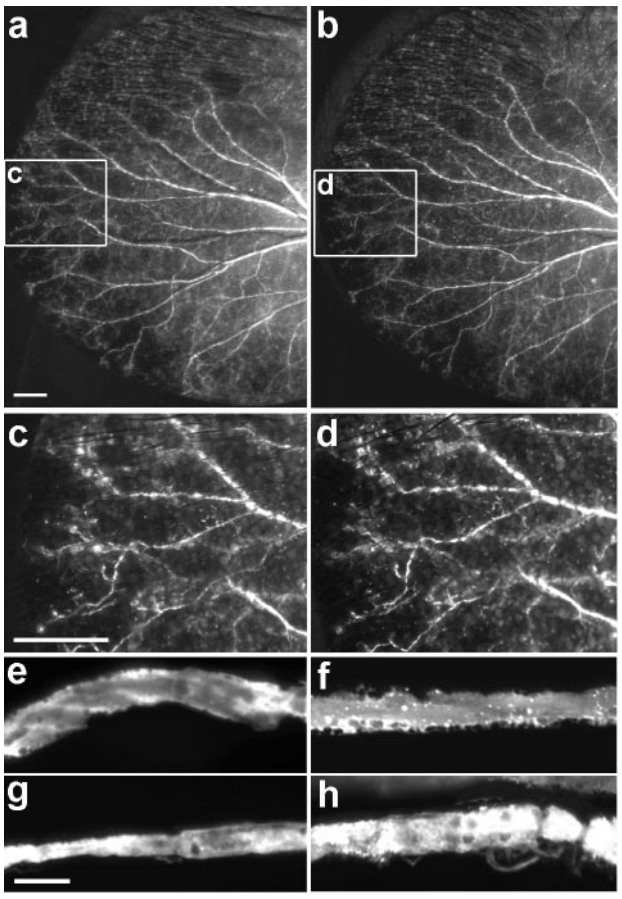

Figure 7. A single dose of vincristine does not cause axonal degeneration. *a–d,* Axons viewed transcutaneously in the pinna of the ear, before and 3 d after administration of vincristine (0.5 mg/kg). The areas boxed in *a* and *b* are shown at higher power in *c* and *d*. *e, f,* Confocal images of dorsal cutaneous axons from intact nerves (*e*, *f*) or proximal segments of crushed nerves (*g*, *h*) in untreated (*e*, *g*) or vincristine-treated (0.5 mg/kg) (*f*, *h*) mice. Scale bars: *a*, *c*, 1 mm; *f*, 10 μm.

Interaction of FK506 and vincristine

FK506 is an inhibitor of calcineurin that was initially introduced into clinical practice as an immunosuppressant but was later reported to enhance functional recovery after peripheral axotomy (Lyons et al., 1994; Gold et al., 1995; Wang et al., 1997; Lee et al., 2000; for review, see Gold and Villafranca, 2003); however, whether the functional effect reflects an ability to speed axonal growth has not been decided. We therefore used YFP transgenic mice to reexamine the effect of FK506 on regeneration.

We assayed regeneration using both the saphenous and dorsal cutaneous nerves, as described above. FK506 was injected daily at 2 mg/kg, a dose shown previously to enhance functional recovery after nerve crush (Wang et al., 1997). We also tested the effect of 5 mg/kg FK506 injected daily on regeneration in the saphenous. FK506 had no detectable effect on regeneration in the saphenous at either dose, suggesting that the rate of regeneration of the fastest-growing axons was not enhanced by FK506 (Fig. 8*a*). In contrast, there was a modest speeding of regeneration in the dorsal cutaneous (Fig. 8*b*,*c*). The difference between the two results suggests that FK506 speeds the average but not the maximum rate of regeneration in a population of axons. Indeed, as in the saphenous, the fastest-growing axons in the dorsal cutaneous did not regenerate faster in the presence of FK506 than in its absence.

Finally, we asked whether FK506 could ameliorate the detrimental effect of vincristine. We combined a submaximal single dose of vincristine (0.125 mg/kg) with daily injections of FK506 and then measured regeneration in the dorsal cutaneous nerves. In fact, FK506 significantly attenuated the effects of vincristine in two respects: the average length of axonal outgrowth was 32% higher in the presence of FK506 than in its absence, and the fraction of axons that failed to regenerate at all was lower in the presence of FK506 than in its absence (11 vs 23%). In both respects, the behavior of axons treated with both FK506 and vincristine was similar to that of control axons that received neither drug (Fig. 8*b*,*c*).

Discussion

The indelible labeling of peripheral sensory axons in XFP transgenic mice provides a new way to analyze their degeneration and regeneration after damage. This method has several advantages

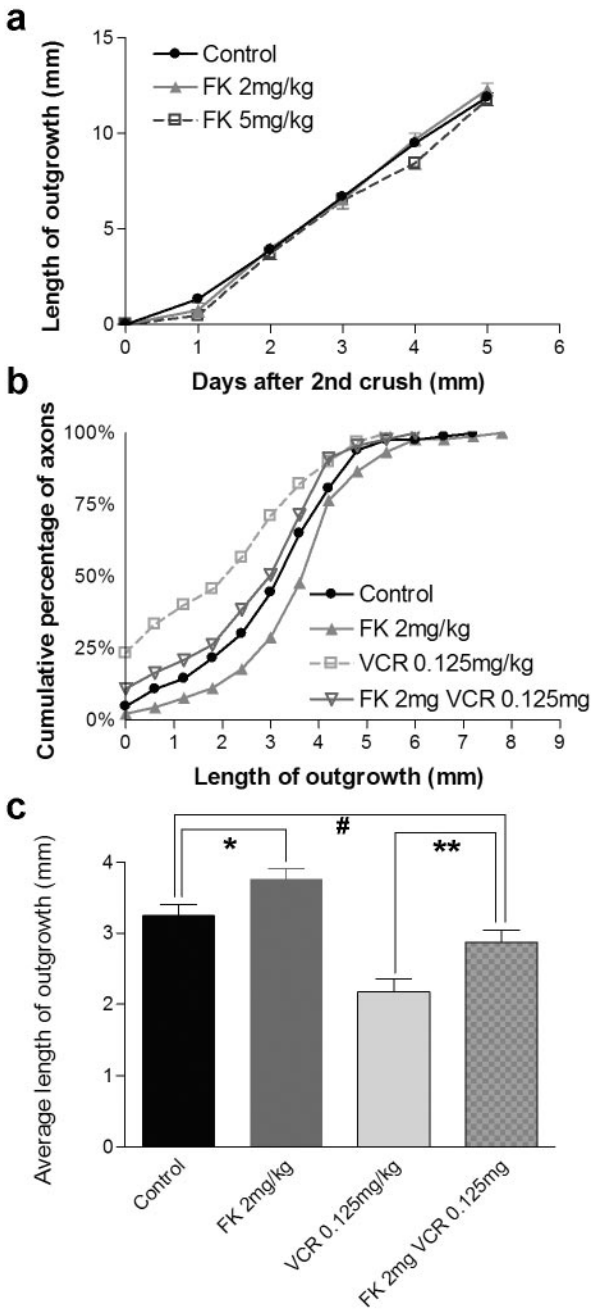

Figure 8. FK506 reverses inhibition of regeneration by vincristine. *a,* Extent of regeneration in the saphenous nerve of mice that received daily doses of FK506. Measurements were made as shown in Figure 4*d–g*. The points and bars show mean ± SEM ($n = 7–10$). FK506 has no significant effect on regeneration in this assay, which measured the regenerative rate of the fastest-growing axons. *b,* Cumulative frequency plot of single axons in dorsal cutaneous nerves from animals that received a single dose of vincristine (VCR), daily administration of FK506, or both. Measurements were made as shown in Figure 3, *i* and *j*. $n = 83–91$ axons per treatment. FK506 modestly speeds regeneration rate. The difference between vincristine and FK plus VCR is significant at $p < 0.05$ by Kolmogorov–Smirnov test. *c,* Mean lengths of regenerating axons from data in *b*. Significance of differences, calculated by *t* test, were $^{*}p = 0.03$; $^{**}p = 0.005$; $^{\#}p > 0.1$.

over previous approaches, which relied on behavioral assays of recovery, electrophysiological recording of action potentials, histological analysis of fixed material, or radiometric assay of axonally transported proteins (see Introduction). First, because the label is visible transcutaneously, time-lapse imaging of degeneration and regeneration is possible *in vivo*. Second, transcutaneous visibility of the nerves makes it possible to damage them through a small incision and monitor them noninvasively, minimizing indirect effects of surgical trauma on the degenerative and regenerative processes. Third, long stretches of individual axons can be imaged in whole mounts of small nerves, facilitating measurements of axonal morphology, branching, and caliber. Fourth, low-power time-lapse and high-power confocal images of the same nerves can be compared. Fifth, the rates of regeneration measured directly in this assay are much less variable from animal to animal than those inferred from behavioral measurements, perhaps because they are more objective. Finally, the assays are not difficult. The transgenic mice can be obtained from a nonprofit source (The Jackson Laboratory), and most measurements can be made with readily available equipment. Together, these features will make it easier to study the behavior of regenerating axons and their responses to treatments that accelerate or inhibit regeneration.

Degeneration and regeneration after nerve cut or crush

Using these methods, we conducted two groups of studies. In one, we compared degeneration and regeneration after three different types of injury: nerve transection, nerve crush, and a crush injury inflicted 3 d after an initial crush injury (the conditioning lesion) at the same site. In general, our results are consistent with those of classical studies. For example, the main histological features of Wallerian degeneration were described in detail more than a century ago (Ramon y Cajal, 1928); the superior regeneration after crush as opposed to transection injury has been noted both in experimental animals and in clinical practice (Young, 1942; Dagum, 1998; Nguyen et al., 2002); the rates of regeneration that we measured (2.4–2.8 mm/d after the initial waiting period) are similar to those reported previously (2.5–4.5 mm/d) (Gutmann et al., 1942; Guth, 1956; Griffin and Hoffman, 1993); and the effect of conditioning lesion has been documented in numerous studies and also replicated *in vitro* (McQuarrie et al., 1977; Forman et al., 1980; Sjoberg and Kanje, 1990; Lankford et al., 1998). The agreement of our results with previous ones, coupled with the novel features of our assay, encourage the view that it will now be possible to reexamine degeneration and regeneration to shed new light on their cellular bases.

In this regard, three observations are noteworthy. First, the ovoids that form in the distal stump during Wallerian degeneration are generally described as being composed primarily of degenerating myelin (Stoll et al., 1989; Griffin and Hoffman, 1993; Hirata et al., 1999). Indeed, although neurofilament-like immunoreactivity has been reported to persist in the distal stump for several days after nerve damage (Bignami et al., 1981), the ovoids are usually visualized with stains for myelin; however, the fact that the ovoids are YFP positive indicates that they are composed to a considerable extent of axonal remnants. Because YFP is a soluble protein, it would be lost rapidly unless it was in a membrane-bound compartment. One possibility is that the YFP is confined to lysosomes or other degradative organelles in Schwann cells or macrophages that had phagocytized the axons. This seems unlikely, however, in light of the large size of the YFP-positive structures. Other possibilities include axonal segments, the membranes of which have resealed, or large axonal fragments that have been fully encapsulated by Schwann cells.

Second, because YFP is easily seen in whole mounts, we were able to observe numerous fine axons extending from the site of transection (Fig. 3*g*). Such escaped fibers were illustrated by Ramon y Cajal et al. (1928), but their number and length may

have been underestimated because they are so easily lost during dissection.

Third, the extent to which rates of regeneration vary among axons has not been appreciated, primarily for technical reasons: most previous assays sample either many axons or the fastest-growing axons in a nerve. In contrast, we were able to measure many axons individually. After a single crush of the dorsal cutaneous nerves, for example, the length of outgrowth varied 10-fold among axons after 5 d (Fig. 5*b*). Such variation has important implications for assessment of factors that influence regeneration rates (see below). Additional analysis will be needed to test whether the differences are primarily in waiting period or regeneration rate and whether the differences vary systematically with axon diameter or modality. Despite the variation, however, it appears that a conditioning lesion affects the entire axon population (Fig. 5*c*).

Vincristine and FK506

For initial studies of pharmacological agents that affect nerve regeneration, we focused on vincristine and FK506 because both are of considerable clinical importance. Vincristine is a potent chemotherapeutic agent, but its efficacy is compromised by the need to limit its dose to avoid side effects, a principal one being peripheral neuropathy (Bradley et al., 1970; Quasthoff and Hartung, 2002). Vincristine neurotoxicity occurs in rodent models but has been difficult to study because it appears only after chronic administration (Apfel et al., 1993; Aley et al., 1996; Tanner et al., 1998). In contrast, a single dose of vincristine slows recovery of sensory and motor function after nerve damage (Nakamura et al., 2001; Paydarfar and Paniello, 2001), suggesting that it impedes axonal regeneration. We have shown directly that this is indeed the case. Moreover, we find that vincristine affects axonal regeneration in two ways. First, vincristine causes some axons to fail to regenerate completely. Second, vincristine slows down the axons that are able to regenerate (Fig. 6*g*). Importantly, the effect of vincristine is rapid but transient: after a single dose, regeneration commences with a delay of 3–4 d (Fig. 6*e*).

Although recovery after peripheral nerve injury is common, it is often slow or incomplete. Therefore, there has been considerable interest in agents that might enhance the speed or completeness of nerve regeneration. The immunosuppressive drug FK506 was the first of a class that has been called the "neuroimmunophilin ligands" on the basis of their resemblance to the immunophilins ligands and their ability to promote functional recovery after peripheral axotomy (Wang et al., 1997; Lee et al., 2000). Whether FK506 also speeds the rate of axon regeneration per se has been less clear (Udina et al., 2002). Our results indicate that there is an increase in the average rate of regeneration without affecting the rate at which the fastest-growing axons regenerate (Fig. 8*b*). This result may explain the lack of effect seen in assays that measure the "front" of regeneration and therefore are most sensitive to the maximal rather than the average rate of regeneration within a nerve. Nonetheless, the effect is modest, indicating that the behavioral improvement noted in other studies may result in large part from other effects of FK506, such as its abilities to increase the caliber of regenerating axons and the rate with which they are remyelinated (Wang et al., 1997; Lee et al., 2000).

Despite the modest effect of FK506 on regeneration after nerve crush, it can greatly attenuate the neurotoxic effect of vincristine (Fig. 8*b*,*c*). There has been great interest in identifying compounds that could counteract this disturbing side effect of vincristine, thereby allowing higher doses to be used to treat cancer. In animal models, insulin-like growth factor, nerve growth factor, and glia-derived neurotrophic factor have all been shown to have this effect, but they have not been useful in clinical practice because they are difficult to deliver and have troubling side effects of their own (for review, see Quasthoff and Hartung, 2002). In contrast, FK506 is already used clinically. Its obvious drawback is that it is an immunosuppressant. Fortunately, however, FK506 appears to act on immune cells and axons by separate mechanisms, and nonimmunosuppressive analogs have been identified that can promote regeneration (Steiner et al., 1997; Gold and Villafranca, 2003). It will now be important to test whether these nonimmunosuppressive analogs prevent vincristine neuropathy in available rodent models. If so, coadministration of such analogs might allow more effective use of vincristine as a chemotherapeutic agent.

References

Aley KO, Reichling DB, Levine JD (1996) Vincristine hyperalgesia in the rat: a model of painful vincristine neuropathy in humans. Neuroscience 73:259–265.

Apfel SC, Arezzo JC, Lewis ME, Kessler JA (1993) The use of insulin-like growth factor I in the prevention of vincristine neuropathy in mice. Ann NY Acad Sci 692:243–245.

Bignami A, Dahl D, Nguyen BT, Crosby CJ (1981) The fate of axonal debris in Wallerian degeneration of rat optic and sciatic nerves. Electron microscopy and immunofluorescence studies with neurofilament antisera. J Neuropathol Exp Neurol 40:537–550.

Boyd JG, Gordon T (2003) Neurotrophic factors and their receptors in axonal regeneration and functional recovery after peripheral nerve injury. Mol Neurobiol 27:277–324.

Bradley WG, Lassman LP, Pearce GW, Walton JN (1970) The neuromyopathy of vincristine in man. Clinical, electrophysiological and pathological studies. J Neurol Sci 10:107–131.

Cui SS, Yang CP, Bowen RC, Bai O, Li XM, Jiang W, Zhang X (2003) Valproic acid enhances axonal regeneration and recovery of motor function after sciatic nerve axotomy in adult rats. Brain Res 975:229–236.

Dagum AB (1998) Peripheral nerve regeneration, repair, and grafting. J Hand Ther 11:111–117.

Danielsen N, Lundborg G, Frizell M (1986) Nerve repair and axonal transport: outgrowth delay and regeneration rate after transection and repair of rabbit hypoglossal nerve. Brain Res 376:125–132.

Fawcett JW, Keynes RJ (1990) Peripheral nerve regeneration. Annu Rev Neurosci 13:43–60.

Feng G, Mellor RH, Bernstein M, Keller-Peck C, Nguyen QT, Wallace M, Nerbonne JM, Lichtman JW, Sanes JR (2000) Imaging neuronal subsets in transgenic mice expressing multiple spectral variants of GFP. Neuron 28:41–51.

Forman DS, McQuarrie IG, Labore FW, Wood DK, Stone LS, Braddock CH, Fuchs DA (1980) Time course of the conditioning lesion effect on axonal regeneration. Brain Res 182:180–185.

Frykman GK, McMillan PJ, Yegge S (1988) A review of experimental methods measuring peripheral nerve regeneration in animals. Orthop Clin North Am 19:209–219.

Gold BG, Villafranca JE (2003) Neuroimmunophilin ligands: the development of novel neuroregenerative/neuroprotective compounds. Curr Top Med Chem 3:1368–1375.

Gold BG, Katoh K, Storm-Dickerson T (1995) The immunosuppressant FK506 increases the rate of axonal regeneration in rat sciatic nerve. J Neurosci 15:7509–7516.

Griffin JW, Hoffman PN (1993) Degeneration and regeneration in the peripheral nervous system. In: Peripheral neuropathy, Ed 3, Vol 1 (Dyck PJ, Griffin JW, Low PA, Poduslo JF, eds), pp 362–376. Philadelphia: W. B. Saunders.

Guth L (1956) Regeneration in the mammalian peripheral nervous system. Physiol Rev 36:441–478.

Gutmann E, Holubar J (1950) The degeneration of peripheral nerve fibres. J Neurol Neurosurg Psychiat 13:89–105.

Gutmann E, Guttmann L, Medawar PB, Young JZ (1942) The rate of regeneration of nerve. J Exp Biol 19:14–44.

Hirata K, Mitoma H, Ueno N, He JW, Kawabuchi M (1999) Differential

response of macrophage subpopulations to myelin degradation in the injured rat sciatic nerve. J Neurocytol 28:685–695.

Keller-Peck CR, Walsh MK, Gan WB, Feng G, Sanes JR, Lichtman JW (2001) Asynchronous synapse elimination in neonatal motor units: studies using GFP transgenic mice. Neuron 31:381–394.

Kim JE, Bonilla IE, Qiu D, Strittmatter SM (2003) Nogo-C is sufficient to delay nerve regeneration. Mol Cell Neurosci 23:451–459.

Lankford KL, Waxman SG, Kocsis JD (1998) Mechanisms of enhancement of neurite regeneration *in vitro* following a conditioning sciatic nerve lesion. J Comp Neurol 391:11–29.

Lee M, Doolabh VB, Mackinnon SE, Jost S (2000) FK506 promotes functional recovery in crushed rat sciatic nerve. Muscle Nerve 23:633–640.

Lubinska L (1977) Early course of Wallerian degeneration in myelinated fibres of the rat phrenic nerve. Brain Res 130:47–63.

Lyons WE, George EB, Dawson TM, Steiner JP, Snyder SH (1994) Immunosuppressant FK506 promotes neurite outgrowth in cultures of PC12 cells and sensory ganglia. Proc Natl Acad Sci USA 91:3191–3195.

McMurray R, Islamov R, Murashov AK (2003) Raloxifene analog LY117018 enhances the regeneration of sciatic nerve in ovariectomized female mice. Brain Res 980:140–145.

McQuarrie IG, Grafstein B, Gershon MD (1977) Axonal regeneration in the rat sciatic nerve: effect of a conditioning lesion and of dbcAMP. Brain Res 132:443–453.

Meiners S, Mercado ML (2003) Functional peptide sequences derived from extracellular matrix glycoproteins and their receptors: strategies to improve neuronal regeneration. Mol Neurobiol 27:177–196.

Mukouyama YS, Shin D, Britsch S, Taniguchi M, Anderson DJ (2002) Sensory nerves determine the pattern of arterial differentiation and blood vessel branching in the skin. Cell 109:693–705.

Murakami T, Fujimoto Y, Yasunaga Y, Ishida O, Tanaka N, Ikuta Y, Ochi M (2003) Transplanted neuronal progenitor cells in a peripheral nerve gap promote nerve repair. Brain Res 974:17–24.

Nakamura Y, Shimizu H, Nishijima C, Ueno M, Arakawa Y (2001) Delayed functional recovery by vincristine after sciatic nerve crush injury: a mouse model of vincristine neurotoxicity. Neurosci Lett 304:5–8.

Neumann S, Woolf CJ (1999) Regeneration of dorsal column fibers into and beyond the lesion site following adult spinal cord injury. Neuron 23:83–91.

Nguyen QT, Sanes JR, Lichtman JW (2002) Pre-existing pathways promote precise projection patterns. Nat Neurosci 5:861–867.

Paydarfar JA, Paniello RC (2001) Functional study of four neurotoxins as inhibitors of post-traumatic nerve regeneration. Laryngoscope 111:844–850.

Qiu J, Cai D, Dai H, McAtee M, Hoffman PN, Bregman BS, Filbin MT (2002) Spinal axon regeneration induced by elevation of cyclic AMP. Neuron 34:895–903.

Quasthoff S, Hartung HP (2002) Chemotherapy-induced peripheral neuropathy. J Neurol 249:9–17.

Ramon y Cajal S (1928) Degeneration and regeneration of the nervous system. New York: Oxford UP.

Ruigt GS, den Brok MH (1995) Retardation of rat sciatic nerve regeneration after local application of minute doses of vincristine. Cancer Chemother Pharmacol 36:530–535.

Sanes JR, Jessell TM (2000) Formation and regeneration of synapses. In: Principles of neural science, Chap 55 (Kandel ER, Schwartz JH, Jessell TM, eds), pp 1087–1114. New York: Elsevier.

Shiraishi S, Le Quesne PM, Gajree T (1985) The effect of vincristine on nerve regeneration in the rat. An electrophysiological study. J Neurol Sci 71:9–17.

Sjoberg J, Kanje M (1990) The initial period of peripheral nerve regeneration and the importance of the local environment for the conditioning lesion effect. Brain Res 529:79–84.

Steiner JP, Connolly MA, Valentine HL, Hamilton GS, Dawson TM, Hester L, Snyder SH (1997) Neurotrophic actions of nonimmunosuppressive analogues of immunosuppressive drugs FK506, rapamycin and cyclosporin A. Nat Med 3:421–428.

Stoll G, Griffin JW, Li CY, Trapp BD (1989) Wallerian degeneration in the peripheral nervous system: participation of both Schwann cells and macrophages in myelin degradation. J Neurocytol 18:671–683.

Tanner KD, Levine JD, Topp KS (1998) Microtubule disorientation and axonal swelling in unmyelinated sensory axons during vincristine-induced painful neuropathy in rat. J Comp Neurol 395:481–492.

Udina E, Ceballos D, Verdu E, Gold BG, Navarro X (2002) Bimodal dose-dependence of FK506 on the rate of axonal regeneration in mouse peripheral nerve. Muscle Nerve 26:348–355.

Van der Zee CE, Man TY, Van Lieshout EM, Van der Heijden I, Van Bree M, Hendriks WJ (2003) Delayed peripheral nerve regeneration and central nervous system collateral sprouting in leucocyte common antigen-related protein tyrosine phosphatase-deficient mice. Eur J Neurosci 17:991–1005.

Wang MS, Zeleny-Pooley M, Gold BG (1997) Comparative dose-dependence study of FK506 and cyclosporin A on the rate of axonal regeneration in the rat sciatic nerve. J Pharmacol Exp Ther 282:1084–1093.

Young JZ (1942) The functional repair of nervous tissue. Physiol Rev 22: 318–374.